

Sintering behavior, structures and microwave dielectric properties of a rutile solid solution system: $(A_xNb_{2x})Ti_{1-3x}O_2$ (A=Cu, Ni)

Li-Xia Pang · Hong Wang · Di Zhou · Xi Yao

Received: 24 December 2007 / Accepted: 4 April 2008 / Published online: 1 May 2008
© Springer Science + Business Media, LLC 2008

Abstract The sintering behavior, structures and microwave dielectric properties in a rutile solid solution system— $(A_xNb_{2x})Ti_{1-3x}O_2$ (A=Cu, Ni)—were investigated and the samples were prepared by conventional solid state reaction method. Single phase of tetragonal rutile structure has been obtained through the entire range of compositions ($0.02 \leq x \leq 0.20$). The sintering temperature was lowered to 900°C by $(Cu_{x/3}Nb_{2x/3})^{4+}$ substituting for Ti^{4+} in the solid solution. Comparing with that of rutile TiO_2 ($465 \text{ ppm}/^\circ\text{C}$), the temperature coefficient of resonant frequency (TCF) of the rutile solid solution is much lower (about $250 \text{ ppm}/^\circ\text{C}$), and the dielectric constant and the quality factor (Qf value) of the solid solution are about 70–80 and 7,000G Hz. The substitution of $(Cu_{x/3}Nb_{2x/3})^{4+}$ or $(Ni_{x/3}Nb_{2x/3})^{4+}$ for Ti^{4+} in the solid solution improved the microwave dielectric properties of the rutile TiO_2 ceramics.

Keywords Rutile solid solution · Microwave dielectric properties · Sintering behavior

1 Introduction

For dielectric resonator applications, there are three main requirements for the microwave dielectrics. First, the dielectric loss ($\tan\delta$) should be very low. Second, the dielectric constant (ϵ_r) should be high, to aid the miniaturization.

Third, the temperature coefficient of the resonant frequency (TCF) should be approximately zero (a few $\text{ppm}/^\circ\text{C}$). In addition, it is desirable that the TCF be able to be “tuned” by small variations in the composition. Achieving all these three requirements in one material is a formidable problem. Rutile TiO_2 is found in a wide range as dielectric resonator material [1–4]. Templeton et al. [5] reported that the un-doped rutile TiO_2 showed a low Q value ($<2,000$) because of the formation of oxygen vacancies when sintered in air atmosphere or under low oxygen partial pressure. The Q value of rutile TiO_2 could be improved by doping 0.05 mol% Zn^{2+} , Cu^{2+} and so on. Afterwards the modified rutile TiO_2 possesses a high dielectric constant (105) and high quality factor (Q ; 9,200 at 5 GHz), but unfortunately the TCF value is still large ($+465 \text{ ppm}/^\circ\text{C}$) and the sintering temperature is too high (1500°C) to be used for LTCC application [6]. Low temperature sintering and microwave dielectric properties of TiO_2 -rutile system were studied by previous works [7, 8]. Kim et al. [7] reported low temperature sintering and microwave dielectric properties of TiO_2 -CuO system for LTCC devices. The addition of 2wt% CuO could lower the sintering temperature of TiO_2 -rutile ceramic to about 900°C , however the TCF value was still high ($+374 \text{ ppm}/^\circ\text{C}$).

Solid solutions are very common in crystalline materials. A solid solution is basically a crystalline phase which can have variable compositions. Certain material properties such as conductivity and ferromagnetism have often been modified by changing the composition in solid solutions, which can be used to design new materials with specific properties. There are lots of papers [9–12] dealing with the synthesis of solid solutions based on the rutile structures, while just a few papers [13] are based on the microwave dielectric properties of these rutile solid solutions. $Ti_{1-x}Cu_{x/3}Nb_{2x/3}O_2$ ($0 \leq x \leq 0.9$) is a set of these rutile solid solutions [14]. The present work is focused on

L.-X. Pang · H. Wang (✉) · D. Zhou · X. Yao
Electronic Materials Research Laboratory,
Key Laboratory of the Ministry of Education,
Xi'an Jiaotong University,
Xi'an, 710049, China
e-mail: hwang@mail.xjtu.edu.cn

the rutile solid solutions of $(\text{Cu}_x\text{Nb}_{2-x})\text{Ti}_{1-3x}\text{O}_2$ and $(\text{Ni}_x\text{Nb}_{2-x})\text{Ti}_{1-3x}\text{O}_2$. Their phase structures, lattice parameters and microstructures were studied. The microwave dielectric properties and sintering behavior of these solid solutions were reported. The relationship between microwave behaviors and structures of these solid solutions was also discussed.

2 Experimental procedures

The compositions of $(\text{Cu}_x\text{Nb}_{2-x})\text{Ti}_{1-3x}\text{O}_2$ and $(\text{Ni}_x\text{Nb}_{2-x})\text{Ti}_{1-3x}\text{O}_2$ were prepared by conventional solid state reaction method using high purity reagent-grade raw materials of CuO (>99%, Guo-Yao Co. Ltd., Shanghai, China), NiO (>99%, Guo-Yao Co. Ltd., Shanghai, China), Nb_2O_5 (>99%, Zhu-Zhou Harden Alloys Co., Ltd., China) and rutile TiO_2 (>99%, Guang Dong Zhaoqing, China). The raw materials were weighted according to the compositions of $(\text{Cu}_x\text{Nb}_{2-x})\text{Ti}_{1-3x}\text{O}_2$ ($x=0.02, 0.05, 0.10, 0.15$, marked as CNT1#~CNT4# for short) and $(\text{Ni}_x\text{Nb}_{2-x})\text{Ti}_{1-3x}\text{O}_2$ ($x=0.05, 0.10, 0.15, 0.20$, marked as NNT1#~NNT4# for short) and milled using a planetary mill (Nanjing Machine Factory, China) with zirconia balls (2 mm in diameter) as milling media. The mixtures were then calcined at 850°C for 12 h to form the rutile solid solution. After being re-milled for 5 h using ZrO_2 balls in deionized water, the powders were pressed into cylinders (6 mm in diameter and 3 mm in height) in a steel die under monoaxial pressure of 20 kN/cm^2 . The cylinders were sintered in air at $870\text{--}1360^\circ\text{C}$ for 8 h.

The phase structures of the samples were investigated using an X-ray diffractometry with $\text{CuK}\alpha$ radiation (Rigaku D/MAX-2400 X-ray diffractometry, Japan). Accurate lattice parameters of the solid solutions were calculated from the XRD patterns obtained by step

scanning measurement. The apparent densities were measured by Archimedes' method. The microstructures of the sintered surface and fracture surface of $(\text{Cu}_x\text{Nb}_{2-x})\text{Ti}_{1-3x}\text{O}_2$ ceramics and $(\text{Ni}_x\text{Nb}_{2-x})\text{Ti}_{1-3x}\text{O}_2$ ceramics were observed by scanning electron microscopy (SEM; JSM-6360LV, JEOL, Japan) coupled with energy-dispersive X-ray spectroscopy (EDS). The dielectric behaviors at microwave frequency of the samples were measured by the $\text{TE}_{01\delta}$ shielded cavity method with a network analyzer (8720ES, Agilent, USA) and a temperature chamber (DELTA 9023, Delta Design, USA). The TCF was calculated by the following formula:

$$TCF = \frac{f_{85} - f_{25}}{f_{25}(85 - 25)} \quad (1)$$

Where f_{85} and f_{25} were the $\text{TE}_{01\delta}$ resonant frequencies at 85°C and 25°C , respectively.

3 Results and discussions

Figure 1 presents the XRD patterns for the powders of $\text{Cu}_x\text{Nb}_{2-x}\text{Ti}_{1-3x}\text{O}_2$ (CNT) ceramics and $\text{Ni}_x\text{Nb}_{2-x}\text{Ti}_{1-3x}\text{O}_2$ (NNT) ceramics. Single phase of tetragonal rutile structure was detected through the entire range of compositions. That is to say rutile solid solution was synthesized by conventional solid state reaction method through the entire range of compositions. In both CNT and NNT solid solution, as x value increasing, the diffraction peaks of rutile phase shifted to lower angle as shown in the inserts of Fig. 1. It indicates that the unit cell volume of the solid solution increased as the x value increasing. The lattice parameters and theoretic bulk density calculated from XRD patterns of $(\text{A}_x\text{Nb}_{2-x})\text{Ti}_{1-3x}\text{O}_2$ ($\text{A}=\text{Cu}$ or Ni) ceramics are shown in Table 1. The lattice parameters (both a value

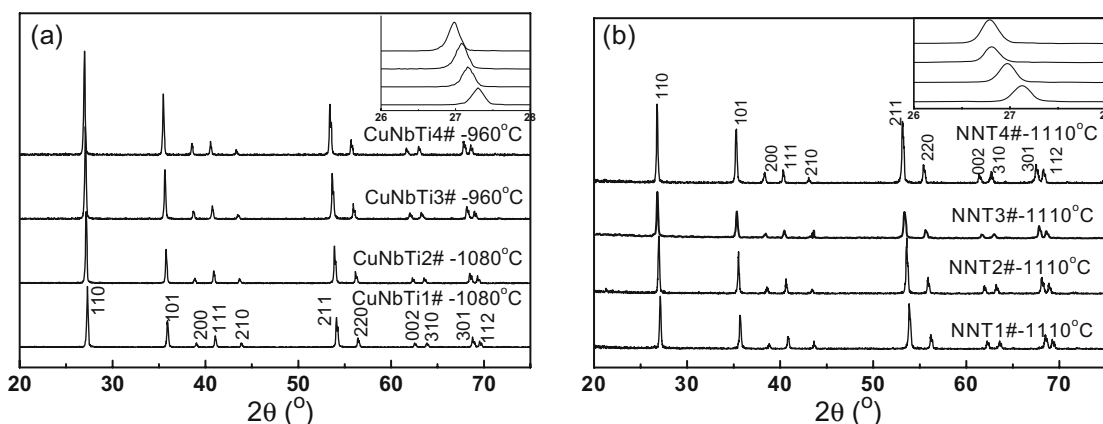


Fig. 1 XRD patterns for powders of (a) $\text{Cu}_x\text{Nb}_{2-x}\text{Ti}_{1-3x}\text{O}_2$ (CNT) ceramics and (b) $\text{Ni}_x\text{Nb}_{2-x}\text{Ti}_{1-3x}\text{O}_2$ (NNT) ceramics

Table 1 Lattice parameters and theoretic bulk density obtained from XRD patterns of $(A_xNb_{2x})Ti_{1-3x}O_2$ ($A=Cu$ or Ni) ceramics in Fig. 1.

| Sample | ST (°C) | <i>a</i> (Å) | <i>c</i> (Å) | <i>c/a</i> | Vol (Å ³) | <i>d</i> calc (g/cm ³) |
|--------|----------|------------------|------------------|------------|-----------------------|------------------------------------|
| CNT1# | 1080/8 h | 4.59984±0.000704 | 2.96471±0.000598 | 0.64450 | 62.73 | 4.3420 |
| CNT2# | 1080/8 h | 4.61927±0.000384 | 2.97334±0.00032 | 0.64368 | 63.44 | 4.4589 |
| CNT3# | 960/8 h | 4.63695±0.000614 | 2.98553±0.000521 | 0.64386 | 64.19 | 4.6803 |
| CNT4# | 960/8 h | 4.65555±0.000614 | 3.00174±0.000552 | 0.64477 | 65.06 | 4.8875 |
| NNT1# | 1110/8 h | 4.61815±0.000952 | 2.97671±0.000814 | 0.64457 | 63.49 | 4.4434 |
| NNT2# | 1110/8 h | 4.64079±0.000796 | 2.99072±0.000667 | 0.64444 | 64.41 | 4.6394 |
| NNT3# | 1110/8 h | 4.65990±0.000875 | 3.00205±0.000701 | 0.64423 | 65.19 | 4.8426 |
| NNT4# | 1110/8 h | 4.67843±0.000897 | 3.01325±0.00076 | 0.64407 | 65.95 | 5.0386 |

and *c* value), unit cell volume and theoretic bulk density were increased as the *x* value increasing in both CNT and NNT solid solutions. The average ionic radius of $(Cu_{x/3}Nb_{2x/3})^{4+}$ (0.67 Å) and $(Ni_{x/3}Nb_{2x/3})^{4+}$ (0.657 Å) are bigger than that of Ti^{4+} (0.605 Å) at the same coordination number [15]. That might be partially responsible for the results.

The bulk densities of CNT ceramics and NNT ceramics as a function of sintering temperature are shown in Fig. 2. The bulk density of $Cu_{0.02}Nb_{0.04}Ti_{0.94}O_2$ (CNT1#) ceramics reached maximum at 990°C, and the relative density of $Cu_{0.02}Nb_{0.04}Ti_{0.94}O_2$ sintered at 990°C for 8 h was as high as 98%. That is to say a small amount of $(Cu_{x/3}Nb_{2x/3})^{4+}$ substituting for Ti^{4+} decreased the sintering temperature effectively from 1500°C to 990°C. CuO is a low melting point oxide and it can lower the sintering temperature of ceramics in two ways. One is acting as a sintering aid [5] and the other is acting as a raw material and forming a composition that containing Cu^{2+} [16]. In the present work, CuO lowered the sintering temperature in the latter way. The sintering temperature of CNT solid solution was lowered to 900°C when the *x* value increased to 0.1, and the sintering temperature was very important for LTCC application. The bulk densities of NNT ceramics increased as the sintering temperature increasing because of the decreasing of the porosity, and they all reached constant when the sintering temperature increased to 1110°C. That indicates all the NNT ceramics

could be densified well since 1110°C and the densified sintering temperature was not much influenced by the content of the substitution of $(Ni_{x/3}Nb_{2x/3})^{4+}$ for Ti^{4+} . For both CNT ceramics and NNT ceramics, the bulk densities increased as the content of the substitution of $(Cu_{x/3}Nb_{2x/3})^{4+}$ and $(Ni_{x/3}Nb_{2x/3})^{4+}$ for Ti^{4+} respectively (as shown in Fig. 2), because theoretic bulk density of CNT ceramics and NNT ceramics increased with the content of the substitution, as shown in Table 1.

Figure 3 illustrates the SEM micrographs of the fracture surface of $Cu_xNb_{2x}Ti_{1-3x}O_2$ (CNT) ceramics sintered at 900–960°C for 8 h and $Ni_xNb_{2x}Ti_{1-3x}O_2$ (NNT) ceramics sintered at 1110°C for 8 h. Alveolate microstructure was obtained in the $Cu_{0.02}Nb_{0.04}Ti_{0.94}O_2$ (CNT1#) ceramic which was sintered at 960°C and the grain size was just 0.5–1 μm. The grains of CNT2# ceramic sintered at 960°C and CNT4# ceramics sintered at both 900°C and 960°C were distributed uniformly in the dense microstructures, respectively, as shown in Fig. 3. For CNT ceramics, the grain size was sensitive to sintering temperature. For example, the average grain size of CNT4# ceramic increased greatly from 1 to 5 μm as the sintering temperature increased from 900°C to 960°C. Compared with that of CNT2# (2.5–3 μm), the average grain size of CNT4# sintered at the same sintering temperature (960°C) increased to about 5 μm. That is to say the average grain size increased as the content of substitution of $(Cu_{x/3}Nb_{2x/3})^{4+}$ for Ti^{4+} increasing. It indicates again that

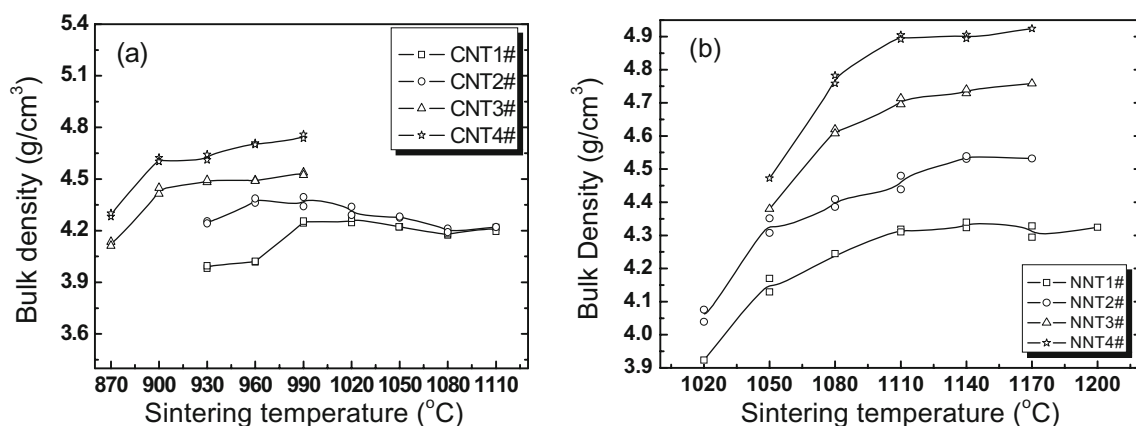


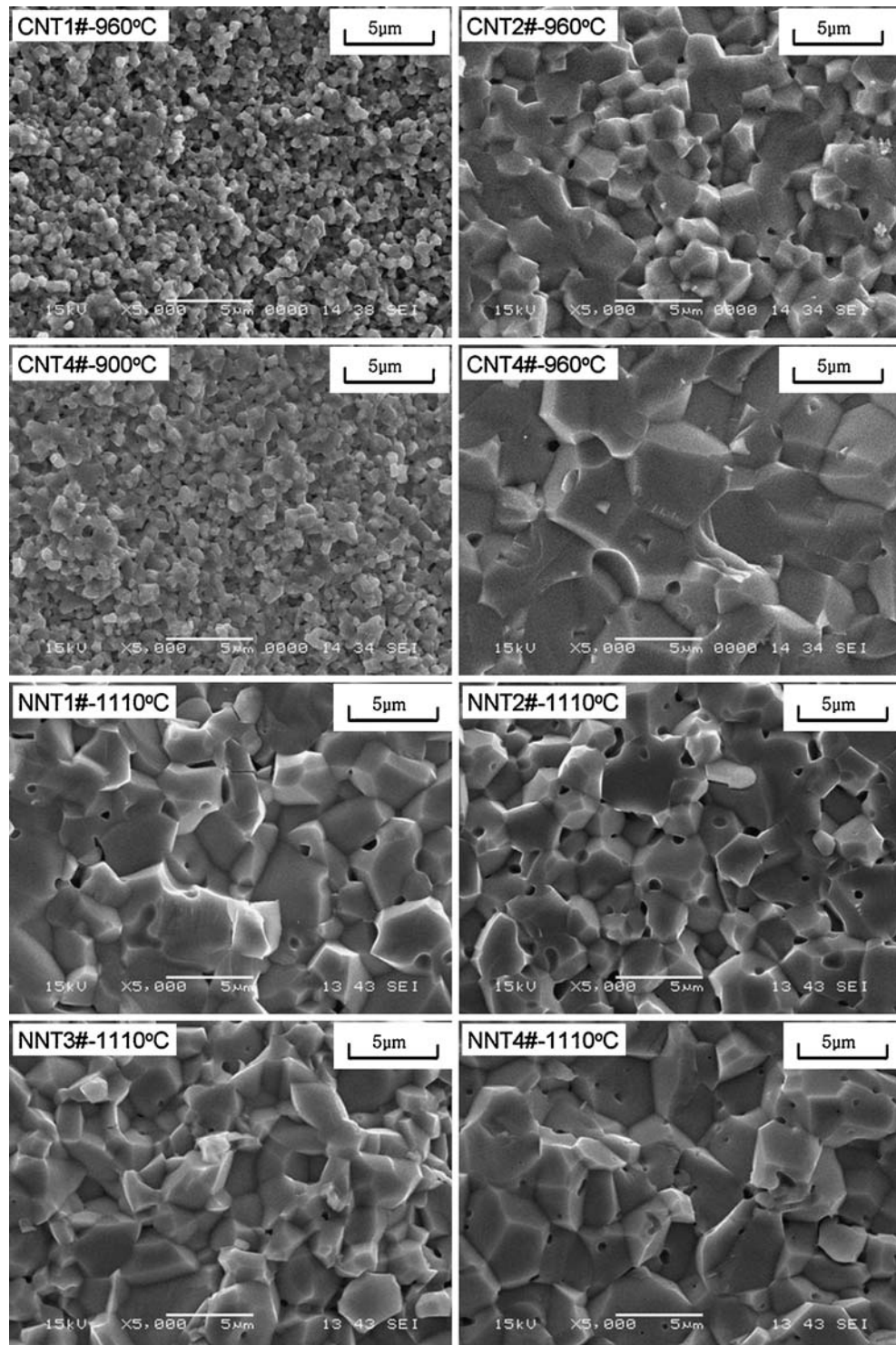
Fig. 2 Bulk densities of (a) $Cu_xNb_{2x}Ti_{1-3x}O_2$ (CNT) ceramics and (b) $Ni_xNb_{2x}Ti_{1-3x}O_2$ (NNT) ceramics as a function of sintering temperature

the substitution of $(\text{Cu}_{x/3}\text{Nb}_{2x/3})^{4+}$ for Ti^{4+} could lower the sintering temperature of the solid solution. The SEM micrographs of NNT ceramics those were sintered at 1110°C also showed dense microstructures. The grains distributed uniformly in the ceramic and there were little pores in the grain boundaries with the average grain sizes of NNT ceramics of $2\sim 5\ \mu\text{m}$. It implied that all the NNT

ceramics were well densified at 1110°C and the sintering temperature depended little on the content of the substitution of $(\text{Ni}_{x/3}\text{Nb}_{2x/3})^{4+}$ for Ti^{4+} .

The microwave dielectric properties (dielectric constant and Qf value) of $\text{Cu}_x\text{Nb}_{2x}\text{Ti}_{1-3x}\text{O}_2$ (CNT) ceramics and $\text{Ni}_x\text{Nb}_{2x}\text{Ti}_{1-3x}\text{O}_2$ (NNT) ceramics as a function of sintering temperature are shown in Fig. 4. The dielectric

Fig. 3 SEM micrographs of fracture surface of $\text{Cu}_x\text{Nb}_{2x}\text{Ti}_{1-3x}\text{O}_2$ (CNT) ceramics sintered at $900\sim 960^\circ\text{C}$ for 8 h and $\text{Ni}_x\text{Nb}_{2x}\text{Ti}_{1-3x}\text{O}_2$ (NNT) ceramics sintered at 1110°C for 8 h



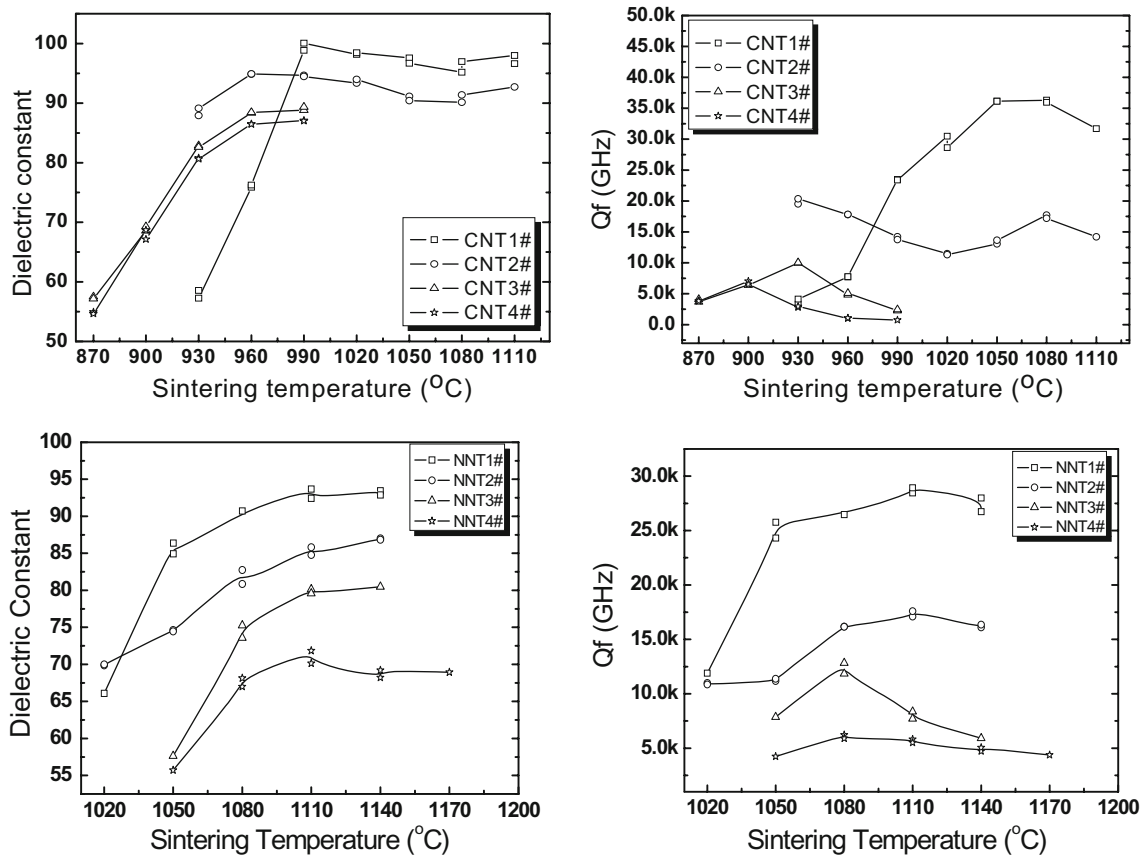


Fig. 4 Microwave dielectric properties of $\text{Cu}_x\text{Nb}_{2x}\text{Ti}_{1-3x}\text{O}_2$ (CNT) ceramics and $\text{Ni}_x\text{Nb}_{2x}\text{Ti}_{1-3x}\text{O}_2$ (NNT) ceramics as a function of sintering temperature

constants of both CNT and NNT ceramics decreased as the contents of substitution of $(\text{Cu}_{x/3}\text{Nb}_{2x/3})^{4+}$ or $(\text{Ni}_{x/3}\text{Nb}_{2x/3})^{4+}$ for Ti^{4+} increasing, although the ionic polarizability of $(\text{Cu}_{x/3}\text{Nb}_{2x/3})^{4+}$ (4.04 \AA^3) and $(\text{Ni}_{x/3}\text{Nb}_{2x/3})^{4+}$ (7.03 \AA^3) are higher than Ti^{4+} (2.93 \AA^3) [17]. It was due do that the dielectric constant of rutile TiO_2 system depends mainly on the structure [18]. Comparing with that of pure rutile TiO_2 (105), the dielectric constants of $\text{Cu}_{0.15}\text{Nb}_{0.3}\text{Ti}_{0.55}\text{O}_2$ ceramic sintered at 990°C and $\text{Ni}_{0.2}\text{Nb}_{0.4}\text{Ti}_{0.4}\text{O}_2$ ceramic sintered at 1110°C were 86 and 71, respectively. The Qf values of both CNT and NNT ceramics also decreased as the contents of substitution of $(\text{Cu}_{x/3}\text{Nb}_{2x/3})^{4+}$ or $(\text{Ni}_{x/3}\text{Nb}_{2x/3})^{4+}$ for Ti^{4+} increasing. Comparing with pure rutile TiO_2 showing a low Q value ($<2,000$) [5], a small amount of substitution of $(\text{Cu}_{x/3}\text{Nb}_{2x/3})^{4+}$ or $(\text{Ni}_{x/3}\text{Nb}_{2x/3})^{4+}$ for Ti^{4+} increased the Qf value of the rutile solid solution. The Qf values of $\text{Cu}_{0.02}\text{Nb}_{0.04}\text{Ti}_{0.94}\text{O}_2$ ceramic sintered at 1050°C and $\text{Ni}_{0.05}\text{Nb}_{0.1}\text{Ti}_{0.85}\text{O}_2$ ceramic sintered at 1110°C were 36,000 GHz and 29,000 GHz, respectively, as shown in Fig. 4. The Qf values of CNT ceramics and NNT ceramics decreased to 7,000 GHz (sintered at 900°C for 8 h) and 12,800 GHz (sintered at 1080°C for 8 h) respectively when the x value increased to 0.15.

Figure 5 shows the temperature coefficients of resonant frequencies (TCF) of $\text{Cu}_x\text{Nb}_{2x}\text{Ti}_{1-3x}\text{O}_2$ (CNT) ceramics and $\text{Ni}_x\text{Nb}_{2x}\text{Ti}_{1-3x}\text{O}_2$ (NNT) ceramics as a function of x value. The TCF values of both CNT and NNT ceramics shifted towards negative as the contents of substitution of $(\text{Cu}_{x/3}\text{Nb}_{2x/3})^{4+}$ or $(\text{Ni}_{x/3}\text{Nb}_{2x/3})^{4+}$ for Ti^{4+} increasing. Comparing with the pure rutile TiO_2 showing a TCF value of

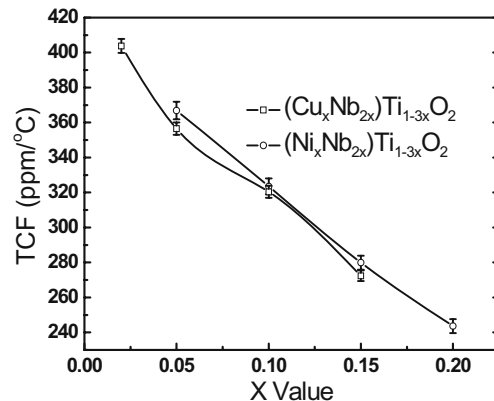


Fig. 5 Temperature coefficients of resonant frequencies (TCF) of $\text{Cu}_x\text{Nb}_{2x}\text{Ti}_{1-3x}\text{O}_2$ (CNT) ceramics and $\text{Ni}_x\text{Nb}_{2x}\text{Ti}_{1-3x}\text{O}_2$ (NNT) ceramics as a function of x value

465 ppm/°C [6], the TCF values of $\text{Cu}_{0.15}\text{Nb}_{0.3}\text{Ti}_{0.55}\text{O}_2$ ceramic sintered at 900°C and $\text{Ni}_{0.2}\text{Nb}_{0.4}\text{Ti}_{0.4}\text{O}_2$ ceramic sintered at 1110°C were +272.4 ppm/°C and +243.6 ppm/°C respectively. The result showed that the substitution of $(\text{Cu}_{x/3}\text{Nb}_{2x/3})^{4+}$ or $(\text{Ni}_{x/3}\text{Nb}_{2x/3})^{4+}$ for Ti^{4+} in the solid solution made a great progress in the system of rutile TiO_2 ceramics for LTCC application since the TCF value of the material should be near to zero for LTCC application.

4 Conclusions

A rutile solid solution system— $(\text{A}_x\text{Nb}_{2x})\text{Ti}_{1-3x}\text{O}_2$ (A=Cu, Ni)—was investigated. Complete rutile solid solution structure was formed through the entire range for both $\text{Cu}_x\text{Nb}_{2x}\text{Ti}_{1-3x}\text{O}_2$ (CNT) ceramics and $\text{Ni}_x\text{Nb}_{2x}\text{Ti}_{1-3x}\text{O}_2$ (NNT) ceramics. The sintering temperature was lowered to 900°C by the $(\text{Cu}_{x/3}\text{Nb}_{2x/3})^{4+}$ substituting for Ti^{4+} in the solid solution. Comparing with that of rutile TiO_2 (465 ppm/°C) and TiO_2 –CuO system (+374 ppm/°C), the temperature coefficient of resonant frequency (TCF) of the rutile solid solution CNT4# ceramic is much lower (about 272.4 ppm/°C), while the dielectric constant and the quality factor (Qf value) of the solid solution are about 70 and 7000 GHz respectively. The substitution of $(\text{Cu}_{x/3}\text{Nb}_{2x/3})^{4+}$ for Ti^{4+} in TiO_2 solid solution made a great progress in the system of rutile TiO_2 ceramics for LTCC application. $\text{Ni}_{0.15}\text{Nb}_{0.3}\text{Ti}_{0.55}\text{O}_2$ ceramic sintered at 1080°C for 8 h showed microwave dielectric properties of $\epsilon_r \sim 75$, Qf~12,800 GHz and TCF~280 ppm/°C as a candidate as high K (ϵ_r) microwave dielectric.

Acknowledgement This work was supported by the National 863-project of China (2006AA03Z0429), National 973-project of China (2002CB613302) and NCET-05-0840.

References

1. K. Wakino, T. Nishikawa, H. Tamura, T. Sudo, *Microwave J*, 133–150 (1987), June
2. Y. Konishi, *Proc. IEEE* **79**(6), 726–740 (1991)
3. W. Wersing, *Curr. Opin. Solid State Mater. Sci* **1**(5), 715–731 (1996)
4. K. Wakino, *Ferroelectrics* **91**, 69–86 (1989)
5. A. Templeton, X. Wang, S.J. Penn, S.J. Webb, L.F. Cohen, N.M. Alford, *J. Am. Ceram. Soc* **83**(1), 95–100 (2000)
6. K. Fukuda, R. Kitoh, I. Awai, *Jpn. J. Appl. Phys* **32**, 4584–4588 (1993)
7. D-W. Kim, B. Park, J-H. Chung, K.S. Hong, *Jpn. J. Appl. Phys* **39**, 2696 (2000)
8. C-K. Shin, Y-K. Paek, *Int. J. Appl. Ceram. Technol* **3**, 463 (2006)
9. B. Khazai, R. Kershaw, K. Dwight, A. Wold, *Mater. Res. Bull* **16**, 655–658 (1981)
10. J.A. Garcia, M.E. Villafuerte-castrejon, J. Andrade, R. Valenzuela, A.R. West, *Mater. Res. Bull* **19**, 649–654 (1984)
11. J. Andrade, M.E. Villafuerte-Castrejon, R. Valenzuela, A.R. West, *J. Mater. Sci. Lett* **5**(2), 147–149 (1986)
12. I. Abrahams, P.G. Bruce, W.I.F. David, A.R. West, *Chem. Mater* **1**, 237–240 (1989)
13. W.S. Kim, J.H. Kim, J.H. Kim, K.H. Hur, J.Y. Lee, *Mater. Chem. Phys* **79**, 204–207 (2003)
14. A. Grandin, M.M. Borel, C. Michel, B. Raveau, *Mater. Res. Bull* **18**, 239–246 (1983)
15. R.D. Shannon, *Acta Crystallogr., Sect. A* **32**, 751 (1976)
16. D. Zhou, H. Wang, X. Yao, *Mater. Chem. Phys* **104**, 397–402 (2007)
17. R.D. Shannon, *J. Appl. Phys* **73**, 348 (1993)
18. R. Coelho, *Physics of Dielectrics for the Engineer* (Elsevier Scientific, Amsterdam, 1979)